Chemical Papers (2023) 77:2679–2687
https://doi.org/10.1007/s11696-022-02657-4

ORIGINAL PAPER

# Synthesis of new trisubstituted hexahydro-isoindole-1,3-dione derivatives regio- and stereoselectivity: spectroscopic and theoretical studies

**Özlem Gündoğdu**[1]

Received: 24 October 2022 / Accepted: 28 December 2022 / Published online: 6 January 2023


**Abstract**
2-Hydroxy-5-alkylhexahydro-4*H*-oxireno[2,3-e]isoindole-4,6(5*H*)-diones were synthesized, and their C-2 selective ring-opening products were obtained through nucleophilic additions such as with MeOH. The methoxydiols obtained from the ring-opening reactions were converted to corresponding acetate derivatives. The structures of the methoxydiacetates were determined by $^{1}H$ and $^{13}C$ NMR and X-ray analyses. Furthermore, theoretical computations were carried out to explain the regioselectivity in the ring-opening reaction of epoxy alcohols. The theoretical calculations showed that the ring-opening reaction of epoxy alcohols proceeds in a thermodynamically controlled manner and regioselectivity occurs depending on the stability of the intermediate.

**Graphical Abstract**

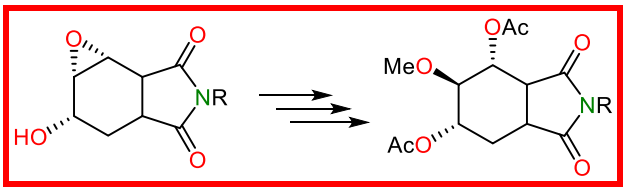


**Keywords** Isoindole-1,3-diones · Ring-opening reaction · Thermodynamically controlled · Regioselectivity · Epoxy alcohol

## Introduction

Norcantharimides, known as isoindole derivatives, are important in terms of several biological activities (Galvis et al. 2013; Lamie et al. 2015). They have been reported to be inhibitors of serine/threonine protein phosphates 1 and 2A (PP1 and PP2A) (Galvis et al. 2013; Hill et al. 2007a, b; Robertson et al. 2011). Isoindole dione derivatives have been the focus of attention as members of an important class of organic compounds with medicinal and biological activities (Scheme 1).

The isoindole skeleton structure consists of a fused five-membered imide and a six-membered ring. Therefore, derivatization may be performed by transformations of both rings to synthesize derivatives of isoindoles. Thus, different functional groups may be included in the nitrogen atom of the imide or the cyclohexane ring.

In a study conducted in 2011 by Tan et al., a new method was developed to incorporate various functional groups into the cyclohexane ring (Tan et al. 2011). These transformations were achieved by two main reactions. The first one was peroxygenation via singlet oxygen and the other one was derivatization of the double bond via addition reactions. For example, isoindoles containing cyclohexene rings were transformed into new derivatives using singlet oxygen and then bromination (Tan et al. 2020), hydroxylation (Tan et al. 2014), and epoxidation reactions (Tan et al. 2014). In addition, the ring-opening reaction of the epoxy

✉ Özlem Gündoğdu
ogundogdu@ahievran.edu.tr

[1] Vocational School of Kaman, Kırşehir Ahi Evran University, 40300 Kırşehir, Turkey

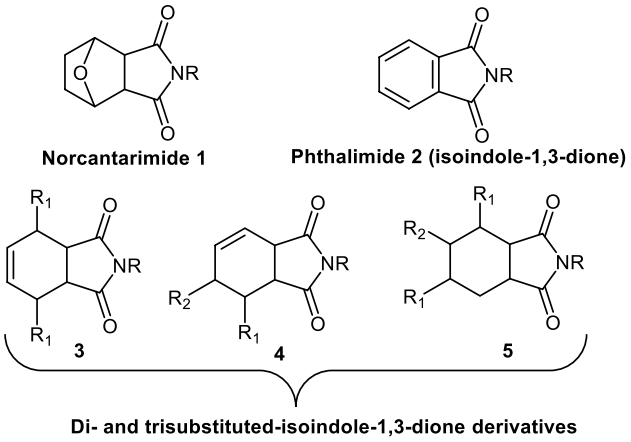


**Scheme 1** Molecular structures of some isoindole-1,3-dione derivatives

alcohol derivatives of isoindoles converted them to various isoindole-1,3-dione derivatives using strong or moderate nucleophiles such as $Br^-$, $Cl^-$, and $N_3^-$ (Scheme 2). Following similar procedures, the C-2 regioselective ring-opening reaction of 2,3-epoxy alcohols with nucleophiles was carried out and the mechanism for the formation of the C-2 regioselective product was supported by theoretical calculations (Gündoğdu et al. 2022).

In the present study, the effects of the structure of the nucleophile and reaction conditions on regioselectivity in the reaction mechanism were investigated using a different approach.

## Experimental

### General

Column chromatography: Silica gel 60 (70–230 mesh) and analytical thin layer chromatography (TLC): Silica gel 60 F254. All of the reagents used in the experiments are commercially available unless otherwise specified, and all solvents were distilled before use. NMR data were recorded on Varian 400 and Bruker 400 spectrometers. $^1H$ and $^{13}C$ NMR spectra were recorded in $CDCl_3$ referenced according to the signals of deuterated solvents. Elemental analysis was performed on a Leco CHNS-932 instrument. Melting point was measured with a Gallenkamp melting point device. X-ray: Rigaku R-AXIS RAPID IP diffractometer. HR-MS: electron spray technique ($M^+/M^-$) from the soln. in MeOH (Waters LCT Premier TM XE UPLC/MS TOF (Manchester, UK)).

### (5*S*)-5-hydroxy-2-alkyl-3a,4,5,7a-tetrahydro-1*H*-isoindole-1,3(2*H*)-dione (11)

Allyl alcohols **11** were synthesized as described in the literature (Tan et al. 2011, 2014, 2016; Gündoğdu et al. 2022).

### General procedure for epoxy alcohols 6

To a solution of allyl alcohol **11** (1.0 g, 5.12 mmol) in $CH_2Cl_2$ (25 mL) was added 77–79% *m*-CPBA (1.49 g, 6.66 mmol) at 0 °C. The reaction was allowed to slowly warm to room temperature for 6 h with stirring. After this period, the reaction mixture was evaporated under reduced pressure. The resulting residue was purified by column chromatography with EtOAc–petroleum ether (40:60), providing **6** (Gündoğdu et al. 2022).

### General procedure for ring opening of epoxy alcohols 6

Allyl epoxide derivatives **6a–b** (1 mmol) were dissolved in MeOH (5 mL). After the addition of three drops of conc. $H_2SO_4$ (98%), the reaction mixture was magnetically stirred at room temperature overnight. The reaction mixture was removed under reduced pressure and proceeded to the next step without purification. The crude product was dissolved in $Ac_2O$ (5 mL) and pyridine (2 mmol) was added. Then, the reaction mixture was magnetically stirred at room temperature for 18 h. The $Ac_2O$ was removed under reduced pressure. The crude product was purified by column chromatography from EtOAc/petroleum ether to give diacetate derivatives **14a–b**.

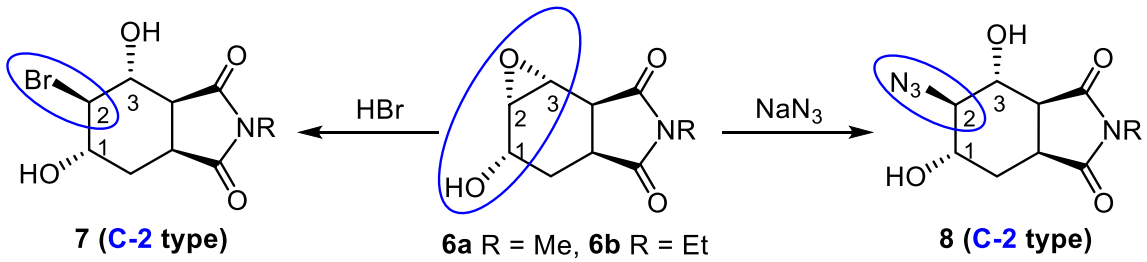


**Scheme 2** The ring-opening reaction of epoxy alcohol **6** with $Cl^-$, $Br^-$, and $N_3^-$

**(4*R*,5*R*,6*S*)-rel-5-methoxy-2-methyl-1,3-dioxooctahydro-1*H*-isoindole-4,6-diyl diacetate (14a):**

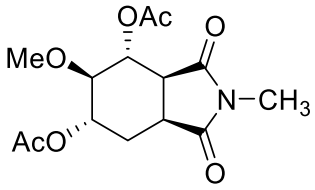


Compound **14a** was obtained as a white solid crystal in 82% yield (mp: 134–135 °C). $^{1}$H NMR (400 MHz, $CDCl_3$) $\delta$ 5.42 [quasi t, $J = 4.8$ Hz, 1H (H-C5)], 4.96 [ddd, $J = 7.3$, 5.3, 2.1 Hz, 1H (H-C7)], 3.47 [dd, $J = 4.8$, 2.1 Hz, 1H (H-C6)], 3.39 (s, 3H, $OCH_3$), 3.18–3.11 (m, 1H, H-C9), 3.08–3.02 (m, 1H, H-C4), 2.98 (s, 3H, N-$CH_3$), 2.29–2.19 (m, 1H, H-C8), 2.13–2.05 (m, 1H, H-C8), 2.13 (s, 3H, $COCH_3$), 2.03 (s, 3H, $COCH_3$). $^{13}$C NMR (100 MHz, $CDCl_3$) $\delta$ 178.20 (CO–NR), 175.34 (CO–NR), 169.55 (O–C=O), 169.53 (O–C=O), 78.92 (CH–$OCH_3$), 69.82 (CH–O), 68.56 (CH–O), 58.33 (O–$CH_3$), 41.59 (CH–C=O), 35.72 (CH–C=O), 25.01 (N–$CH_3$), 23.73 ($CH_2$), 20.98 ($COCH_3$), 20.95 ($COCH_3$). **HRMS**: (ESI), *m/z*: $[M + H]^+$ Calcd. for $C_{14}H_{19}NO_7 + H^+$ 314.1240; Found, 314.1199.

**(4*R*,5*R*,6*S*)-rel-2-ethyl-5-methoxy-1,3-dioxooctahydro-1*H*-isoindole-4,6-diyl diacetate (14b):**

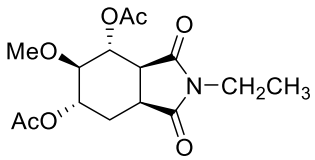


Compound **14b** was obtained as a yellow liquid in 80% yield. $^{1}$H NMR (400 MHz, $CDCl_3$) δ 5.24 [t, $J = 4.6$ Hz, 1H (H-C5)], 4.77 [ddd, $J = 7.3$, 5.3, 2.1 Hz, 1H (H-C7)], 3.38 (dd, $J = 7.2$ Hz, 2H, N-$CH_2$), 3.31 [dd, $J = 4.5$, 2.2 Hz, 1H (H-C6)], 3.23 (s, 3H, $OCH_3$), 3.04–2.89 (m, 2H, H-C9 and H-C4), 2.19–2.11 (m, 1H, H-C8), 2.05–1.95 (m, 1H, H-C8), 1.98 (s, 3H, $COCH_3$), 1.93 (s, 3H, $COCH_3$), 0.99 (t, $J = 7.2$ Hz, 3H, –$CH_2CH_3$). $^{13}$C NMR (100 MHz, $CDCl_3$) $\delta$ 177.86 (CO–NR), 174.98 (CO–NR), 169.42 (O–C=O), 169.40 (O–C=O), 79.10 (CH–$OCH_3$), 69.81 (CH–O), 68.60 (CH–O), 57.99 (O–$CH_3$), 41.45 (CH–C=O), 35.66 (CH–C=O), 33.74 (N–$CH_2$), 23.62 ($CH_2$), 20.86 ($COCH_3$), 20.79 ($COCH_3$), 12.37 (N–$CH_3$). **HRMS**: (ESI), *m/z*: $[M + H]^+$ Calcd. for $C_{15}H_{21}NO_7 + H^+$ 328.1396; Found, 328.1368.

## X-ray crystallography

For the crystal structure determination, a single crystal of the molecule methoxydiacetate **14a** was used for data collection on a four-circle Rigaku R-AXIS RAPID-S diffractometer (equipped with a two-dimensional area IP detector). Graphite-monochromated Mo-$K_\alpha$ radiation ($\lambda = 0.71073$ Å) and oscillation scans with $\Delta w = 5°$ for one image were used for data collection. The lattice parameters were determined by the least-squares methods on the basis of all reflections with $F^2 > 2\sigma(F^2)$. Integration of the intensities, correction for Lorentz and polarization effects, and cell refinement were performed using CrystalClear (Rigaku/MSC Inc., 2005) software. The structures were solved by direct methods using SHELXS-97, which allowed for the location of most of the heaviest atoms, with the remaining non-hydrogen atoms being located from different Fourier maps calculated from successive full-matrix least-squares refinement cycles on $F^2$ using SHELXL-97 (Sheldrick 1997). All non-hydrogen atoms were refined using anisotropic displacement parameters. Hydrogens attached to carbons were located at their geometric positions using appropriate HFIX instructions in SHELXL. The final difference Fourier maps showed no peaks of chemical significance. *Crystal data for* **14a:** $C_{14}H_{19}NO_7$, crystal system, space group: monoclinic, Cc; (no:9); unit cell dimensions: $a = 12.9529(8)$, $b = 14.9548(9)$, $c = 7.7563(5)$ Å, $\alpha = 90$, $\beta = 94.540(4)$, $\gamma = 90°$; volume; 1497.7(3) Å$^3$, $Z = 4$; calculated density: 1.390 g/cm$^3$; absorption coefficient: 0.112 mm$^{-1}$; $F(000)$: 664; $\theta$-range for data collection 2.0°–28.8°; refinement method: full-matrix least-square on $F^2$; data/parameters: 3536/204; goodness-of-fit on $F^2$: 1.123; final $R$-indices $[I > 2\sigma(I)]$: $R_1 = 0.034$, w$R_2 = 0.102$; largest diff. peak and hole: 0.307 and −0.347 e Å$^{-3}$.

CCDC-2177439 contains the supplementary crystallographic data for this structure (**3**). These data are provided free of charge via the joint CCDC/FIZ Karlsruhe deposition service www.ccdc.cam.ac.uk/structures.

## Results and discussion

The starting material, 2-alkyl-3a,4,7,7a-tetrahydro-1*H*-isoindole-1,3(2*H*)-dione (**9**), was prepared by Diels–Alder reaction of 3-sulfolene and maleic anhydride followed by the reaction of condensation with a primary amine ($MeNH_2$, $EtNH_2$) (Tan et al. 2011, 2014, 2016; Gündoğdu et al. 2022). In the next step, the cyclohexene moiety of compound **9** was converted to the corresponding hydroperoxide. For this purpose, compound **9**

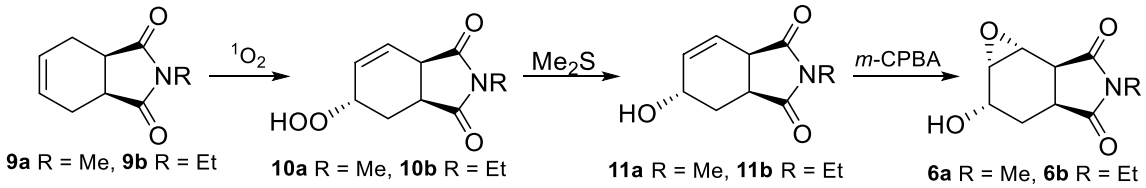


**Scheme 3** Synthesis of epoxy alcohols

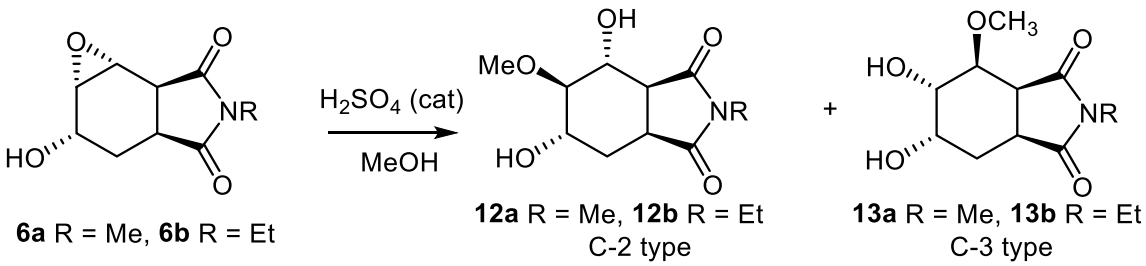


**Scheme 4** The ring-opening reaction of epoxy alcohols **6a–b** and the structure of C-2 and C-3 type isomers

was subjected to an ene reaction of singlet oxygen to give the corresponding hydroperoxides (**10a–b**). The hydroperoxide groups of compounds **10a–b** were then reduced to corresponding allyl alcohol compounds **11a–b** using $Me_2S$. Subsequently, compounds **11a–b** were oxidized with *m*-chloroperbenzoic acid (*m*-CPBA) to give *syn*-epoxy alcohols **6a–b** (Scheme 3). The $^1$H NMR spectrum of the crude product indicated that the epoxides **6a–b** were obtained as the sole products (Scheme 3) (Gündoğdu et al. 2022). It is known that as a result of the treatment of cyclic allylic alcohols with *m*-CPBA, the formation of epoxides occurs on the same side as the hydroxyl group (Hoveyda et al. 1993; Bach et al. 1998; Itoh et al. 1979).

Epoxy alcohols may give interesting ring-opening products with different structures in the form of isomers because they contain three different reactive sites. Therefore, the formation of regio- or stereoselective products in the opening reactions is considered a useful tool for synthesis. Very recently, a C-2 regioselective ring-opening reaction of 2,3-epoxy alcohol **6a** with HX was performed (Gündoğdu et al. 2022). The ring-opening reactions proceed through an $S_N2$-like mechanism. In addition, the regioselectivity observed during the product formation was realized according to the transition state. In this context, in order to examine the effect of nucleophiles and reaction conditions on regioselectivity, it was decided to investigate the ring-opening reactions of epoxy alcohols under different conditions. For this purpose, first the ring-opening reaction of the epoxy alcohol derivative **6** was studied by reacting MeOH in the presence of $H_2SO_4$. Since the structures of the 2,3-epoxy alcohols **6a-b** are asymmetrical, we

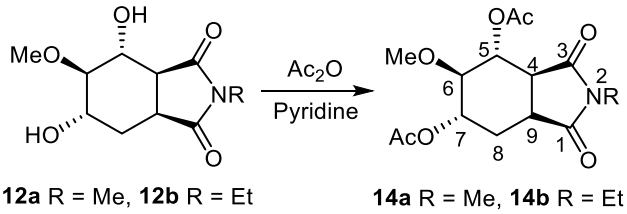


**Scheme 5** The acetylation reaction of methoxydiol **12a–b** with $Ac_2O$

supposed that C-2 and C-3 type isomers could be formed in the ring-opening reaction (Scheme 4).

For easily dissolution of crude product(s) and determine the structure of the formed product(s), **12a–b** were subjected to acetylation to yield **14a–b** (Scheme 5). Analysis of the reaction mixture showed the isomers **14a** and **14b** as sole products in the methanolysis of **6a** and **6b**. The reaction mixture was purified by column chromatography to give **14a–b** in 82% and 80% yields, respectively.

The structure of the methoxydiacetate **14a** was assigned by $^1$H NMR spectroscopy. Proton–proton coupling and proton–carbon correlations were determined using the COSY and HMQC spectra of methoxydiacetate **14a** (Scheme 6).

In the $^1$H NMR spectrum of compound **14a**, the most conspicuous feature is the doublet of doublets of doublets arising from the –C*H*OAc proton resonance at 4.96 ppm. In this case, the C*H*OAc proton at C-7 is adjacent to three chemically non-equivalent protons. Therefore, the C*H*OAc proton H-C (7) is coupled with the $H_2$-C (8) protons and H-C (6) and it is split into a doublet of doublets of doublets. The measured coupling constants $J = 7.3$, 5.3, and 2.1 Hz clearly supported these results. Furthermore, the triplet at 5.96 ppm

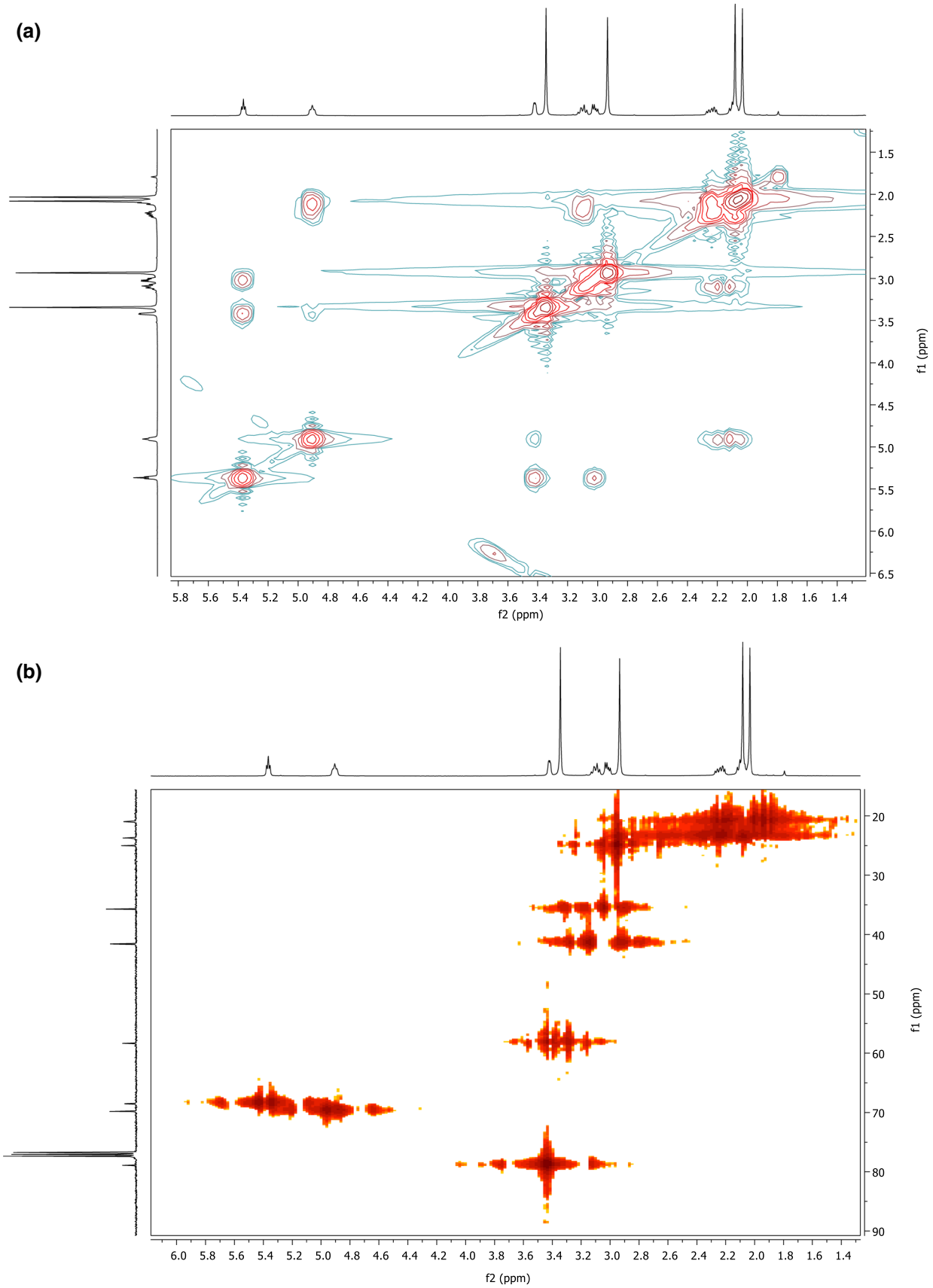


**Scheme 6** **a** COSY NMR spectrum of **14a** and **b** HMQC NMR spectrum of **14a**

belongs to the H-C (5) proton. This proton is adjacent to two other protons, and the coupling constants of these two protons are very close to each other ($J = 4.8$ Hz). The relative positions of the C*H*–OMe (H–C (6)) and C*H*–OAc (H–C (5)) protons in the cyclohexane ring were determined by double resonance experiments. Those experiments clearly indicated that the carbon atom-bearing methoxy group (–C*H*–OMe) was located between the carbon atom-bearing acetoxy groups (SI, Scheme 3).

These results show that the methoxy group is regioselectivity bonded to the C-2 carbon and the C-2 type product **14a** is formed. After determining the positions of the acetoxy and methoxy groups, studies were carried out to determine the configurations of these groups. According to the structure of the epoxy alcohol, the configuration of the acetoxy and methoxy groups in the product can be easily predicted, because products with *trans*-stereochemistry are formed in the ring-opening reaction of epoxide. The methoxy group attached to the C6 carbon is on the other side of the ring with respect to the two acetate groups, and the methoxy group has *trans*-stereochemistry with respect to the acetate groups. It was planned to confirm the predicted configuration using the coupling constants of H-C (5), H-C (6), and H-C (7) protons. For this purpose, the coupling constants of each proton were determined, in particular J values between the H-C (6) and the H-C (5) and H-C (7) protons. The coupling constants between these protons were $J_{5,6} = 4.8$ Hz and $J_{6,7} = 2.1$ Hz. Especially since $J_{6,7}$ is smaller than expected and for *trans*-stereochemistry, it was decided to perform X-ray analysis of the molecule to determine the exact configuration. For this purpose, the structure of isomer **14a** was further confirmed by single-crystal analysis (Fig. 1).

The exact conformation of 5-methoxy-2-methyl-1,3-dioxooctahydro-1*H*-isoindole-4,6-diyl diacetate (**14a**) was confirmed by X-ray diffraction analysis (Fig. 1). Molecule **14a** crystallizes in monoclinic space group *Cc* with four molecules in the unit cell. The cyclohexane unit has a chair conformation with the lowest energy and the C–C (cyclohexane) bond lengths are in the range of 1.518(3)–1.543(3) Å; all have the single bond character. C2–O2 and C3–O1 bond distances are 1.206(3) and 1.204(3) Å, respectively. The structure of racemic bicyclic **14a** has five asymmetric carbon atoms and the stereogenic centers are as follows: C4(*R**), C5(*R**), C7(*R**), C8(*R**), and C9(*S**). In the solid state, the structure stabilized via moderate intermolecular C–H•••O hydrogen bonds [*D*•••*A* = 3.079(3)–3.215(3) Å], which led to each different enantiomer forming a polymeric structure. In addition, vdW interactions contribute the formation of a stable structure. The fact that almost every molecule contributes to the vdW interaction with hydrogen bonding ensures that the molecules are tightly packed (Fig. 1).

After the structure of the C-2 type ring-opening product **14a** was confirmed, $H_2SO_4$ catalyzed methanolysis was also carried out in the epoxy alcohol **6b** bearing –NEt. It was determined from the recorded $^1$H NMR spectrum of the crude product that a single isomer was formed in this reaction. Comparison of the $^1$H and $^{13}$C NMR data of –NEt **14b** with the data of –NMe **14a** showed good agreement, confirming the C-2 type substitution product. Theoretical calculations were carried out to explain the formation of the single isomer in the epoxide ring-opening reaction. In order to better understand the regioselectivity in the reaction between protonated epoxy alcohol and MeOH, theoretical computations were performed. For this purpose, the density functional theory (DFT) and the B3LYP functional (Becke 1993; Lee et al. 1988; Vosko et al. 1980; Stephens et al. 1994) were used. In all the computations, Pople's polarized triple-ζ split valence basis set augmented with diffuse functions, 6-311++ G(d,p) (Hariharan and Pople 1973; McLean and Chandler 1980; Krishnan et al. 1980), was used. Geometry optimization and harmonic vibrational frequency computations were conducted at the B3LYP/6-311G++ (d,p) level. All minimum and transition state structures were optimized in MeOH solvent employing the solvent model density SMD solvation model (Marenich et al. 2009) at the B3LYP/6-311G++ (d,p) level at 298 K and 1 atm. All the computations were performed using the Gaussian 09 software package (Frisch et al. 2013). For the transition state (TS) between species A and B, the A/B notation is used in this study.

As can be seen Scheme 7, two different possible reaction pathways, a and b, can occur with the nucleophilic attack of MeOH on the C-2 or C-3 carbon in the protonated epoxy alcohol **6a**. The reaction pathway including C-3 attack proceeds via the transition state **6a/16a'**, while the other reaction pathway, C-2 attack, carries on via the transition state **6a/15a'**.

According to the computational results, the computed reaction free energy and barrier for the reaction pathway including C-2 attack are -8.6 and 11.2 kcal/mol, respectively (Fig. 2). For the C-3 attack, the computed reaction free energy and barrier are – 10.5 and 12.9 kcal/mol, respectively (Fig. 2). Therefore, the C-2 pathway takes place with a lower reaction barrier by relatively about 2 kcal/mol than that of the C-3 pathway, indicating that the C-2 regioselectivity in the reaction between protonated epoxy alcohol **6a** and MeOH is more favorable. The computational results are in good agreement with the experimental results.

## Conclusions

The synthesis and characterization of novel trisubstituted analogs of isoindole-1,3-diones by ring-opening reaction of epoxy alcohols are reported. In addition, $H_2SO_4$ catalysis and methanolysis of epoxy alcohols **6a–b** were

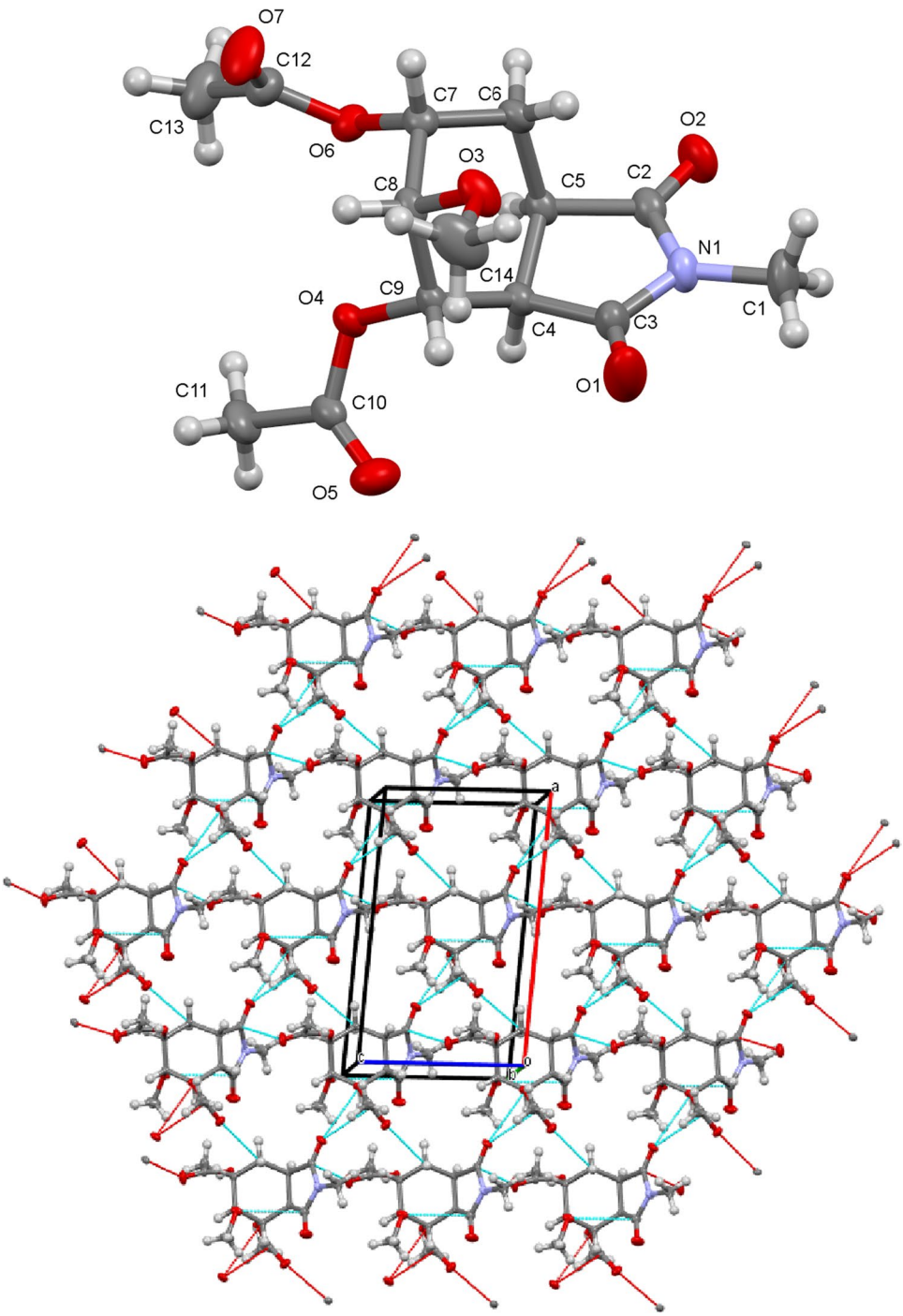


**Fig. 1** (Up) X-ray structure of molecule **14a**. Thermal ellipsoids are drawn at the 40% probability level. (Down) Stacking motif with the unit cell viewed down along the *b*-axis. Dashed red and turquoise lines indicate interactions less than the sum of vdW radii and the H-bonding contacts

performed with extremely high selectivity under mild conditions to give trisubstituted isoindole-1,3-dione derivatives. Moreover, the C-2 regioselective formation of **12a** was explained by theoretical calculations. The results obtained from the ring-opening reactions in which epoxy alcohols give MeOH show that the formation of the products occurs according to the stability of the intermediate. The reagent and reaction conditions used in epoxy alcohol ring-opening reactions are important for regioselectivity. In particular, X-ray analysis of **14a** showed that each molecule in the crystal lattice contributed to the vdW

**Scheme 7** Reaction mechanism for the opening of the protonated epoxy alcohol with MeOH

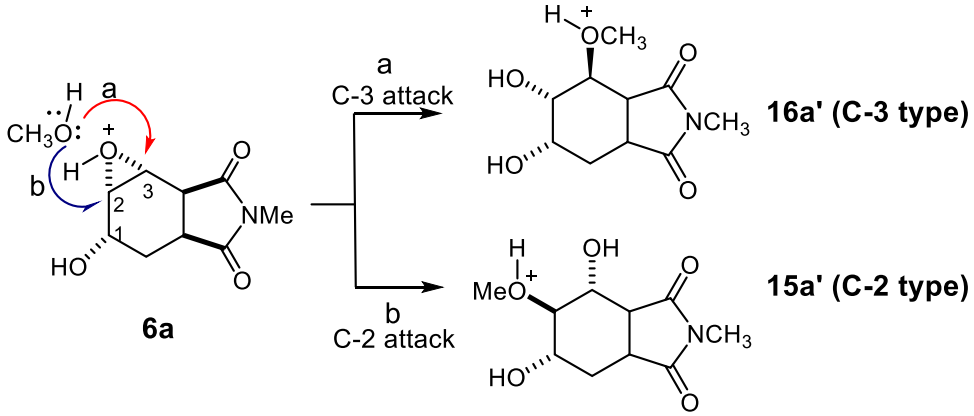


**Fig. 2** Relative free energy profile for the reaction mechanism shown in Scheme 7 computed at the B3LYP/6-311++ G(d,p) level

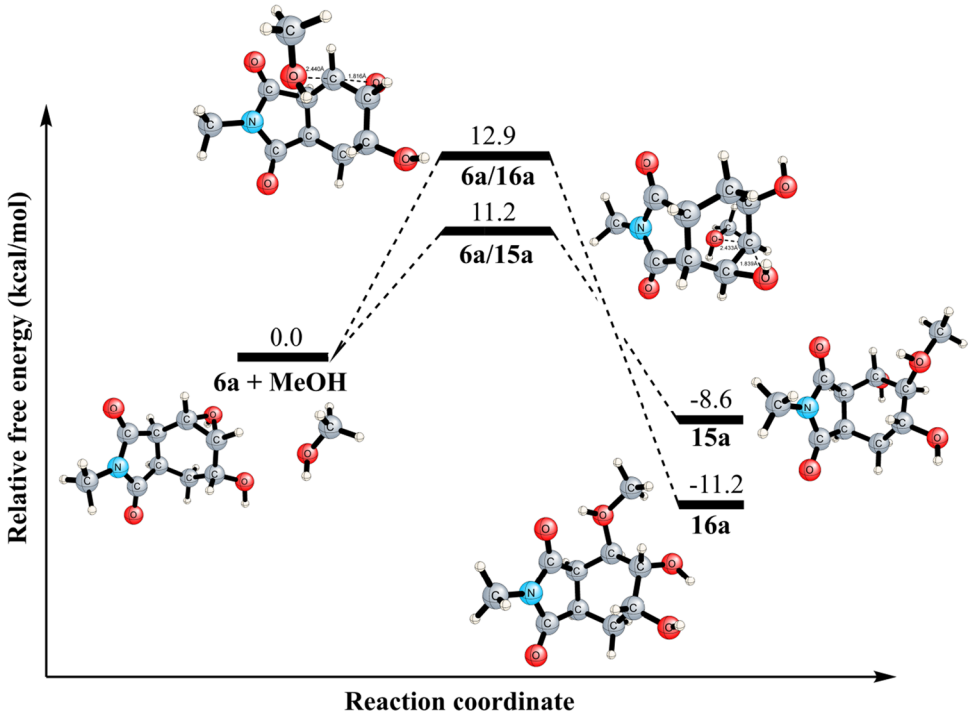


interaction with hydrogen bonding, ensuring the molecules were tightly packed.

**Supplementary Information** The online version contains supplementary material available at https://doi.org/10.1007/s11696-022-02657-4.

**Acknowledgements** The author is grateful to Dr. Ertan Sahin, Dr. Yunus Kara, Dr. Hasan Seçen, and Dr. Abdurrahman Atalay for their valuable contributions and Atatürk University for some of the spectroscopic analysis.

**Declaration**

**Conflict of interest** The author declares that there is no conflict of interest in this article.

## References

Bach RD, Estévez CM, Winter JE, Glukhovtsev MN (1998) On the origin of substrate directing effects in the epoxidation of allyl alcohols with peroxyformic acid. J Am Chem Soc 120:680–685. https://doi.org/10.1021/ja9717976

Becke AD (1993) Density-functional thermochemistry. III. The role of exact exchange. J Chem Phys 98(7):5648–5652. https://doi.org/10.1063/1.464913

Frisch MJ, Trucks GW, Schlegel HB, Scuseria GE, Robb MA, Cheeseman JR, Scalmani G, Barone V, Petersson GA, Nakatsuji H, Li X, Caricato M, Marenich A, Bloino J, Janesko BG, Gomperts R, Mennucci B, Hratchian HP, Ortiz JV, Izmaylov AF, Sonnenberg JL, Williams-Young D, Ding F, Lipparini F, Egidi F, Goings J, Peng B, Petrone A, Henderson T, Ranasinghe D, Zakrzewski VG, Gao J, Rega N, Zheng G, Liang W, Hada M, Ehara M, Toyota K, Fukuda R, Hasegawa J, Ishida M, Nakajima T, Honda Y, Kitao O, Nakai H, Vreven T, Throssel Kl, Montgomery JA, Peralta JE, Ogliaro F, Bearpark M, Heyd JJ, Brothers E, Kudin KN,

Staroverov VN, Keith T, Kobayashi R, Normand J, Raghavachari K, Rendell A, Buran JCT, Iyengar SS, Tomasi J, Cossi M, Millam JM, Klene M, Adam C, Cammi R, Ochtersk JWI, Martin RL, Morokuma K, Farkas O, Foresman JB, Fox DJ (2013) Gaussian 09, Revision D.01. Gaussian, Inc., Wallingford

Galvis P, Carlos E, Leonor Y, Mendez V, Vladimir Kouznetsov V (2013) Cantharidin-based small molecules as potential therapeutic agents. Chem Biol Drug Des 82:477–499. https://doi.org/10.1111/cbdd.12180

Gündoğdu Ö, Atalay A, Çelebioğlu N, Anıl B, Şahin E, Şanlı-Mohamed G, Bozkaya U, Kara Y (2022) Regio- and stereo-chemical ring-opening reactions of the 2,3-epoxy alcohol derivative with nucleophiles: explanation of the structures and C-2 selectivity supported by theoretical computations. J Mol Struct. https://doi.org/10.1016/j.molstruc.2022.133163

Hariharan PC, Pople JA (1973) The influence of polarization functions on molecular orbital hydrogenation energies. Theor Chem Acc 28:213–222. https://doi.org/10.1007/bf00533485

Hill TA, Stewart SG, Ackland SP, Gilbert J, Sauer B, Sakoff JA, McCluskey A (2007a) Norcantharimides, synthesis and anticancer activity: synthesis of new norcantharidin analogues and their anticancer evaluation. Bioorg Med Chem 15:6126–6134. https://doi.org/10.1016/j.bmc.2007.06.034

Hill TA, Stewart SG, Sauer B, Gilbert J, Ackland SP, Sakoff JA, McCluskey A (2007b) Heterocyclic substituted cantharidin and norcantharidin analogues—synthesis, protein phosphatase (1 and 2A) inhibition, and anti-cancer activity. Bioorg Med Chem Lett 17:3392–3397. https://doi.org/10.1016/j.bmcl.2007.03.093

Hoveyda AH, Evans DA, Fu GC (1993) Substrate-directable chemical reactions. Chem Rev 93:1307–1370. https://doi.org/10.1021/cr00020a002

Itoh T, Jitsukawa K, Kaneda K, Teranishi S (1979) Vanadium-catalyzed epoxidation of cyclic allylic alcohols. Stereoselectivity and stereocontrol mechanism. J Am Chem Soc 101:159–160

Krishnan R, Binkley JS, Seeger R, Pople JA (1980) Self-consistent molecular orbital methods. XX. A basis set for correlated wave functions. J Chem Phys 72:650–654. https://doi.org/10.1063/1.438955

Lamie P, Philoppes J, El-Gendy A, Rarova L, Gruz J (2015) Design, synthesis and evaluation of novel phthalimide derivatives as in vitro anti-microbial, anti-oxidant and anti-inflammatory agents. Molecules 20:16620–16642. https://doi.org/10.3390/molecules200916620

Lee C, Yang W, Parr RG (1988) Development of the Colle-Salvetti correlation-energy formula into a functional of the electron density. Phys Rev B 37:785–789. https://doi.org/10.1103/PhysRevB.37.785

Marenich AV, Cramer CJ, Truhlar DG (2009) Universal solvation model based on solute electron density and on a continuum model of the solvent defined by the bulk dielectric constant and atomic surface tensions. J Phys Chem B 113:6378–6396. https://doi.org/10.1021/jp810292n

McLean AD, Chandler GS (1980) Contracted Gaussian basis sets for molecular calculations. I. Second row atoms, Z = 11–18. J Chem Phys 72(10):5639–5648. https://doi.org/10.1063/1.438980

Robertson MJ, Gordon CP, Gilbert J, McCluskey A, Sakoff JA (2011) Norcantharimide analogues possessing terminal phosphate esters and their anti-cancer activity. Bioorg Med Chem 19:5734–5741. https://doi.org/10.1016/j.bmc.2011.01.031

Sheldrick GM (1997) SHELXS-97 and SHELXL-97, program for crystal structure solution and refinement. University of Göttingen, Germany

Stephens PJ, Devlin FJ, Chabalowski CF, Frisch MJ (1994) Ab initio calculation of vibrational absorption and circular dichroism spectra using density functional force fields. J Phys Chem 98:11623–11627. https://doi.org/10.1021/j100096a001

Tan A, Koc B, Sahin E, Kishali NH, Kara Y (2011) Synthesis of new cantharimide analogues derived from 3-sulfolene. Synthesis 7:1079–1084. https://doi.org/10.1055/s-0030-1258466

Tan A, Aktaş D, Gundogdu O, Kazancıoglu M, Sahin E, Kishali NH, Kara Y (2014) Convenient synthesis of new polysubstituted isoindole-1,3-dione analogues. Turk J Chem 38:629–637. https://doi.org/10.3906/kim-1310-30

Tan A, Koc B, Kishali N, Kara Y (2016) Synthesis of new hexahydro-1H-isoindole-1,3(2H)-dione derivatives from 2-ethyl/phenyl-3a,4,7,7a-tetrahydro-1H-isoindole-1,3-(2H)-dione. Turk J Chem 40(5):830–840. https://doi.org/10.3906/kim-1511-66

Tan A, Yaglioglu AS, Kishali NH, Sahin E, Kara Y (2020) Evaluation of cytotoxic potentials of some isoindole-1, 3-dione derivatives on HeLa, C6 and A549 cancer cell lines. Med Chem 16(1):69–77. https://doi.org/10.2174/1573406415666181206115638

Vosko SH, Wilk L, Nusair M (1980) Accurate spin-dependent electron liquid correlation energies for local spin density calculations: a critical analysis. Can J Phys 58:1200–1211. https://doi.org/10.1139/p80-159